

Quantum Chemical Investigation of 1-Aminohomopiperidine in Treatment of Breast Cancer Based on Molecular Docking Strategy

S. JEYAVIJAYAN^{1,*}, M. RAMUTHAI¹ and PALANI MURUGAN²

¹Department of Physics, Kalasalingam Academy of Research and Education, Krishnankoil-626126, India

²Department of Physics, Dr. B.R. Ambedkar Institute of Technology, Port Blair-744103, India

*Corresponding author: E-mail: sjeyavijayan@gmail.com

Received: 8 October 2021;

Accepted: 15 December 2021;

Published online: 10 March 2022;

AJC-20728

The density functional theory DFT-B3LYP strategy is promising technique for investigating the molecular structure, wavenumber assignments and several structural properties. The compounds with piperidine ring were valuable substrates in the development of drugs. Therefore, this work was carried out for 1-aminohomopiperidine (1AHP) with B3LYP/6-311++G(d,p) calculations. Broad frequency analyses, molecular stability interactions and charge exchanges of the molecule have been detailed by natural bond orbital (NBO) analysis. Frontier molecular orbital analysis and the UV absorption have been studied by using DFT method. Furthermore, the molecular docking results exposed that the title molecule has a good binding affinity to the active sites interaction with ER α (estrogen receptor alpha) and used as a potential agent of breast cancer efficacy.

Keywords: 1-Aminohomopiperidine, Frequency assignments, Molecular docking, Breast cancer.

INTRODUCTION

Cancer is considered as an infection having uncontrolled growth of cells and the spread of these irregular cells to other tissues within the body. It may be caused by numerous exterior and interior factors. Genetic mutations, hormonal conditions are the main key to cause cancer [1]. Since last 30 years, the number of new cancer patients and death cases are continuously rising [2,3]. It is difficult to challenge in medical science, due to cancer can influence each tissue within the human body [4-6]. Among these cancers, the foremost common one is breast cancer which affects globally [7-9]. It is considered to be the worldwide fastest malignancy, though there has been tremendous effort to control this cancer. As per research, in 1970 the first breast cancer tissue from a malignant adenocarcinoma was first taken from an old woman. The cells were useful to perform the research on the breast cancer. These studies can be performed *in vitro* as many features of mammary epithelium are retained in the cell line. Hence, many works have centered in the field of pharmaceutical drugs for cancer chemotherapy administration and its lead to different side effects [10].

Piperidine is a heterocyclic family comprising of a six-membered ring that includes five methylene groups (-CH₂-) and one amine group (-NH-). It is originating in barley and black pepper. It is a main part in the different drugs which are of significant interest. It is additionally of prime significance in a few chemical degradation responses, for illustration, DNA sequencing in altered nucleotides cleavage. Recent years, piperidine frameworks have moved into preclinical challenging [11]. It shows numerous biological actions *viz.* a few piperidine covering structures established farnesyl transferase (FT) inhibition, an enzyme that's found to be dynamic in different types of cancer [12].

Recently, many reports based on piperidine derivatives showed biological efficacy and solid inhibition activity against breast cancer marker [13-17]. These innumerable applications of piperidine derivatives were motivated for the theoretical and experimental investigations on 1-aminohomopiperidine (1AHP). From literature report, no computation study has been done on 1AHP molecule as a powerful drug application. In DFT approaches, Becke's three-parameter hybrid function associated with the Lee-Yang-Parr relationship (B3LYP) expects

good calculation for structural analysis [18]. In this study, the structural and electronic excited states related to stability and reactivity of 1AHP has been computed utilizing DFT/B3LYP technique. It is a capable approach for calculating infrared, vibrational wavenumbers, molecular geometries and molecular orbital energies [19]. The present work has also been focused to identify the Mulliken charges and natural bond orbitals (NBO) of 1AHP. Further, molecular docking (MD) has been used in the drug development to provide possible protein-ligand interactions [20]. Thus, the MD investigation has been carried out to confirm the repressive nature of 1AHP against breast cancer related proteins.

EXPERIMENTAL

Fourier transform infrared (FTIR) spectrum of 1-aminohomopiperidine (1AHP) was recorded by Perkin-Elmer FTIR spectrometer equipped with a KBr pellet at room temperature. Stand-alone FT-Raman spectrum of molecule 1AHP was noted by using Bruker RFS 27 model spectrometer at room temperature with a resolution of 2 cm^{-1} . The FTIR and FT-Raman spectra have been recognized in the wavenumber range $4000\text{--}400$ and $4000\text{--}50\text{ cm}^{-1}$, respectively.

Computational studies: The GAUSSIAN 09W program [21] has been exploited for DFT calculations. Initially, the structure of 1-aminohomopiperidine (1AHP) was optimized by the DFT/B3LYP [22,23] approach with a 6-311++G (d,p) then the frequency wavenumbers and intensities are calculated. The scaled quantum mechanical (SQM) [24] method have been used to compare the experimental data and DFT results. Hence, the computed vibrations were scaled by employing a scaling value of 0.9613 for the B3LYP strategy [25]. The frontier molecular orbitals (FMOs) of 1AHP have been visualized by Gaussview 05 visualization program [26]. The UV-Vis region of 1AHP have been calculated (without any solvation) by using time-dependent (TD)-DFT/B3LYP method. The ^{13}C & ^1H NMR shielding was recorded using the Gauge-Invariant-atomic orbital (GIAO) method. The vibrational wavenumbers of each functional group of 1AHP have been confirmed from the potential energy distribution (PED) using MOLVIB program [27].

Protein and ligand structure: In breast cancer care there is main protein marker such as ER α (estrogen receptor alpha) (PDB ID: 1EPG). This protein data is extracted from the site (<http://www.pdb.org>) [28]. We have taken 1AHP as a ligand, and its structure was gotten from the open ligand databases: PubChem (<http://pubchem.ncbi.nlm.nih.gov>). The molecular docking of these protein was performed using the software discovery studio (Adaptation: 2017 R2 client) program to assess the protein structure and amino corrosive location by docking interaction with 1AHP.

Molecular docking: The protein ligand docking was performed using a software Auto dock vina (version 4.2.1) [29]. The configuration file was generated based on the size of box and coordinates on the receptor. The hydrogen and molecular torsions were added to each screened ligand. Pdbqt format is used to calculate the docking binding energy affinities (kcal/mol). Receptors and ligand locations are also saved in same format. There were 10 different docking process generated for

each ligand using the Auto dock vina software. The discovery studio version 2017 R2 Client [30] software was used to check the quantity of hydrogen bonds and non-covalent relations of each complex and also to create interaction maps.

RESULTS AND DISCUSSION

Molecular structure analysis: The most optimized stable structure of 1-aminohomopiperidine (1AHP) is shown in Fig. 1. 1AHP possess C1 point group, contains pyridine ring and its optimized bond lengths N1-C2, N1-C7, N1-N8, N8-H9, N8-H10 have been calculated at 1.462, 1.463, 1.424, 1.019, 1.014 Å, which are in agreement with the corresponding experimental values 1.446, 1.449, 1.442, 0.900, 1.191 Å. Similarly, the other geometrical bond distances are related with the available XRD [31] and are reported in Table-1. From the computed results, most of the bond distances are deduced from the experimental parameters, since theoretical estimate is predicted in the gassy state, whereas the test values were noted in the liquid state. The calculated global least energy for 1AHP is obtained as -346.62726672 Hartrees. The calculated C-C bond distances were ranges from 1.525 to 1.560 Å, which are comparable with the experimental (1.524 -1.549 Å) values. Because of methylene group disorder, the single bond C-C distance diverges slightly from the testified value. The change in bond angles is due to the electronegativity of the nitrogen atom, the existence of lone pair electrons, and the assembly of the double bonds. The carbon atoms show an involvement on the outermost electron of the H atoms demonstrates a significant raise in the C-H force constant and reduces its bond distance. The C-H would be affected by the influences of the inductive-mesomeric relations [32]. The effect of ring can be understood from the rise in bond length of C4-C5 (1.560 by B3LYP and 1.549 Å by experimental). Geometrical parameter could be an efficient tool for describing bond type and studying bond quality. From the DFT results, the C2-N1-C7, C2-N1-N8 and C2-C3-C4 bond angles are oriented as 115.1°, 112.2°, 115.5°, respectively, (Experimental values: 120.0°, 112.3°, 117.4°). All the dihedral angles of the 1AHP ring are also listed in Table-1.

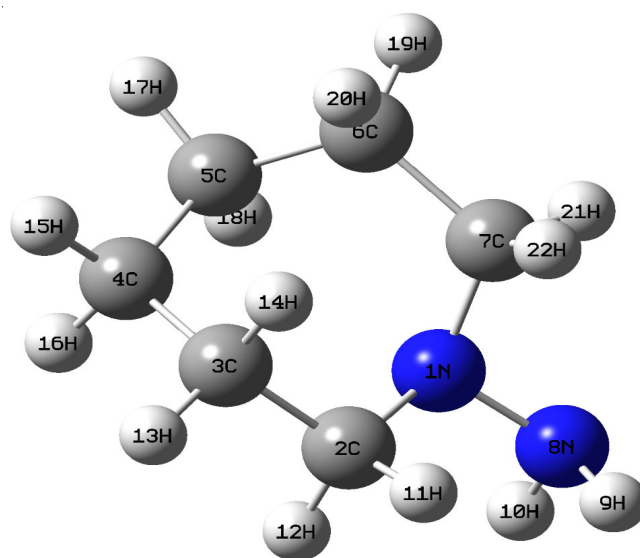


Fig. 1. Optimized structure of 1-aminohomopiperidine (1AHP)

TABLE-1
OPTIMIZED STRUCTURAL PARAMETERS OF 1-AMINOHOMOPIPERIDINE
CALCULATED BY THE DFT/B3LYP METHOD WITH 6-311++G (d,p) BASIS SET

Bond length (Å)	6-311++G (d,p)	Expt. [31]	Bond angle (°)	6-311++G (d,p)	Expt. [31]	Dihedral angles (°)	6-311++G (d,p)	Expt. [31]
N1-C2	1.462	1.446	C2-N1-C7	115.1	120.0	N8-N1-C2-H11	51.4	28.7
N1-7C	1.463	1.449	C2-N1-N8	112.2	112.3	C2-N1-C7-C6	-75.8	-80.7
N1-8N	1.424	1.442	C7-N1-N8	110.1	114.8	C2-N1-C7-H22	49.2	41.5
C2-C3	1.525	1.524	N1-C2-C3	113.7	120.2	N8-N1-C7-H21	36.1	44.9
C2-H11	1.110	0.990	N1-C2-H11	110.3	115.5	C2-N1-N8-H10	76.9	70.5
C2-H12	1.095	0.990	N1-C2-H12	107.1	107.9	C7-N1-N8-H9	88.7	87.7
C3-C4	1.536	1.523	C3-C2-H11	108.5	108.0	N1-C2-C3-C4	47.8	24.7
C3-H13	1.094	0.990	C3-C2-H12	110.0	108.0	N1-C2-C3-H14	-75.5	-85.3
C3-H14	1.093	0.990	H11-C2-H12	106.7	107.6	H11-C2-C3-H13	-66.3	-64.6
C4-C5	1.560	1.549	C2-C3-C4	115.5	117.4	H12-C2-C3-C3	-72.4	-70.5
C4-H15	1.095	0.990	C2-C3-H13	107.6	108.7	C2-C3-C4-H16	65.3	60.4
C4-H16	1.094	0.990	C2-C3-H14	109.1	108.0	H13-C3-C4-H16	-56.2	-59.5
C5-C6	1.536	1.503	C4-C3-H13	109.3	108.0	H14-C3-C4-H15	-56.4	-62.3
C5-H17	1.094	0.990	C4-C3-H14	109.1	108.0	H16-C4-C5-H17	88.0	85.2
C5-H18	1.091	0.990	H13-C3-H14	105.5	108.3			
C6-C7	1.553	1.515	C3-C4-C5	114.6	116.8			
C6-H19	1.093	0.990	C3-C4-H15	107.2	108.6			
C6-H20	1.094	0.990	C3-C4-H16	109.7	108.9			
C7-H21	1.090	0.990	C5-C4-H15	109.3	110.0			
C7-H22	1.106	0.990	C5-C4-H16	109.3	107.2			
N8-H9	1.019	0.900	H15-C4-H16	106.0	107.0			
N8-H10	1.014	1.191	C4-C5-C6	113.8	113.3			
			C4-C5-H17	108.9	108.6			
			C4-C5-H18	109.6	107.4			
			C6-C5-H17	108.8	108.6			
			C6-C5-H18	106.7	108.6			
			H17-C5-H18	114.1	108.6			
			C5-C6-C7	108.6	114.2			
			C5-C6-H19	109.5	116.0			
			C5-C6-H20	108.1	108.6			
			C7-C6-H19	110.1	116.0			
			C7-C6-H20	113.4	107.5			
			H19-C6-H20	104.9	107.5			
			N1-C7-C6	111.4	117.4			
			N1-C7-H21	109.7	108.9			
			N1-C7-H22	110.1	109.0			
			H21-C7-H22	106.6	108.6			
			N1-N8-H9	110.9	111.6			
			N1-N8-H10	108.2	108.6			
			H9-N8-H10	107.5	107.7			

Thermodynamic properties: The thermodynamic limitations of 1AHP are given in Table-2. As the interaction among the atoms within the molecule is very stronger, then the dipole moment will be most extreme. Here, the computed dipole moment and total energy of 1AHP are found as 1.443 Debye and 132.749 kcal mol⁻¹. The irrelevant vibrational energy (zero-point) is obtained (127.57467 kcal mol⁻¹) for 1AHP. These thermodynamic parameters can be employed in the assessment of chemical responses and to notice the further thermodynamic energies of 1AHP.

Vibrational assignments: The studied molecule 1AHP comprises 22 atoms and hence its 60 modes of typical vibrations are dynamic in both spectra (IR and Raman). Figs. 2 and 3 revealed the computed and experimental FTIR and FT-Raman spectra of 1AHP. The IR and Raman peak intensities and the vibrational wavenumbers of 1AHP are given in Table-3.

TABLE-2
THERMODYNAMIC PARAMETERS
OF 1-AMINOHOMOPIPERIDINE

Parameters	Method/basis set 6-311++G (d,p)
Optimized global minimum energy (Hartrees)	-346.62726672
Total energy (thermal), E _{total} (kcal mol ⁻¹)	132.749
Heat capacity, C _v (cal mol ⁻¹ K ⁻¹)	32.104
Total Entropy, S (cal mol ⁻¹ K ⁻¹)	88.028
Translational Entropy (cal mol ⁻¹ K ⁻¹)	40.112
Rotational Entropy (cal mol ⁻¹ K ⁻¹)	28.202
Vibrational Entropy (cal mol ⁻¹ K ⁻¹)	19.714
Vibrational energy, E _{vib} (kcal mol ⁻¹)	130.972
Zero point vibrational energy, (kcal mol ⁻¹)	127.57467
Rotational constants (GHz)	
A	2.952
B	1.787
C	1.350
Dipole moment (Debye)	1.443

TABLE-3
CALCULATED VIBRATIONAL FREQUENCIES (cm^{-1}), IR INTENSITIES (Km mol^{-1}), RAMAN SCATTERING ACTIVITY ($\text{\AA}^4 \text{amu}^{-1}$), REDUCED MASS (amu), FORCE CONSTANTS (mDyne/\AA^{-1}) AND VIBRATIONAL ASSIGNMENTS BASED ON TED PERCENTAGE FOR 1-AMINOHOMOPIPERIDINE

S. No.	Observed wavenumber (cm^{-1})		Wavenumber (cm^{-1})		IR Intensity	Raman activity	Reduced mass	Force constant	Assignment with TED (%)
	FTIR	FT-Raman	Calculated	Scaled					
1	3349(w)	3358(w)	3531	3394	0.7822	90.9628	1.0823	7.9513	vNH _{2ass} (98)
2	3158(vw)	3161(vw)	3354	3224	40.1589	220.5028	1.0582	7.0161	vNH _{2ass} (96)
3	3009(w)	3012(ms)	3107	2988	19.9888	89.4538	1.0880	6.1897	vCH(95)
4	2997(ms)	2999(vs)	3085	2966	49.8586	35.7863	1.0972	6.1539	vCH(94)
5	2964(ms)	–	3060	2942	55.0376	71.3179	1.1010	6.0746	vCH(92)
6	2887(ms)	2888(w)	3053	2935	49.7238	84.1314	1.0984	6.0335	vCH(93)
7	–	2994(vs)	3040	2922	35.9045	146.4893	1.0913	5.9449	vCH(91)
8	–	2878(vw)	3034	2917	43.0104	275.5522	1.0727	5.8209	vCH(92)
9	2858(vw)	–	3026	2909	43.7842	81.7707	1.0665	5.7575	vCH(90)
10	2841(vw)	–	3023	2905	13.1294	48.4100	1.0670	5.7449	vCH(91)
11	–	2832(vw)	3017	2900	35.7004	101.9930	1.0821	5.8041	vCH(90)
12	2782(vw)	–	3010	2894	20.5234	58.9470	1.0623	5.6709	vCH(89)
13	2758(vw)	–	2908	2795	102.5078	123.7258	1.0746	5.3575	vCH(86)
14	2646(vw)	–	2875	2764	98.1558	117.6659	1.0740	5.2307	vCH(87)
15	1522(ms)	1516(w)	1673	1608	18.2388	7.5821	1.0822	1.7851	NH _{2aciss} (85)
16	1498(ms)	1484(ms)	1520	1461	6.5162	3.6573	1.0874	1.4807	vCC(84)
17	1477(w)	–	1501	1443	5.6156	2.5258	1.0922	1.4513	vCC(86)
18	1454(w)	–	1499	1441	7.3304	2.7782	1.0857	1.4390	vCC(84)
19	1409(w)	1412(w)	1496	1438	4.9686	8.1542	1.0832	1.4285	vCC(82)
20	1397(vw)	–	1489	1431	5.6734	8.2168	1.0805	1.4124	vCC(80)
21	1388(w)	1396(w)	1481	1424	1.6281	10.2368	1.0766	1.3913	vCN(83)
22	1357(w)	–	1411	1356	6.4743	3.8169	1.4370	1.6877	vCN(82)
23	–	1348(ms)	1395	1341	5.4198	0.8588	1.3899	1.5950	bCH(80)
24	1349(w)	–	1389	1335	4.8033	1.7997	1.3604	1.5483	bCH(76)
25	–	1327(vw)	1378	1325	0.3460	1.4075	1.2992	1.4550	bCH(78)
26	1315(w)	–	1371	1318	4.7883	2.5622	1.3722	1.5211	bCH(74)
27	1306(w)	1308(w)	1359	1306	0.5217	0.1799	1.3069	1.4222	bCH(72)
28	1276(vw)	–	1343	1291	9.3043	2.9778	1.2790	1.3593	bCH(75)
29	–	1251(vw)	1309	1258	8.2366	6.0815	1.2487	1.2614	bCH(72)
30	1243(w)	1246(vw)	1300	1250	4.7635	8.7620	1.2024	1.1978	vNN(71)
31	1225(vw)	–	1280	1230	1.1877	4.8199	1.1920	1.1521	bCH(75)
32	1202(w)	1204(w)	1257	1208	1.4244	2.3801	1.2663	1.1795	bCH(73)
33	–	1136(w)	1246	1198	4.4224	4.2906	1.5158	1.3871	bCH(72)
34	–	1120(w)	1217	1170	4.9431	2.8263	1.2620	1.1025	bCH(70)
35	1112(ms)	1117(vw)	1186	1140	6.8191	1.5569	2.4975	2.0728	bCH(71)
36	1003(vw)	–	1143	1099	20.1936	4.6633	2.0710	1.5957	NH _{2rock} (70)
37	–	1085(vw)	1122	1079	0.0797	0.8901	1.9432	1.4414	ω CH(69)
38	1048(w)	1039(w)	1102	1059	7.7940	2.7151	2.4220	1.7356	ω CH(65)
39	1006(vs)	1004(vw)	1052	1011	1.6268	5.2475	1.7900	1.1673	ω CH(68)
40	997(ms)	989(w)	1035	995	3.9110	2.3455	1.5801	0.9973	ω CH(69)
41	988(ms)	–	1005	966	11.0275	7.4030	2.2874	1.3635	ω CH(66)
42	913(w)	916(w)	956	919	4.3809	2.6935	2.1605	1.1640	ω CH(65)
43	894(vw)	–	920	884	63.8234	1.9000	1.5671	0.7820	ω CH(64)
44	–	859(vw)	908	873	21.1912	0.8720	1.9141	0.9318	ω CH(63)
45	837(ms)	842(w)	866	832	4.4712	1.6237	2.6833	1.1877	ω CH(65)
46	815(vw)	–	856	823	6.2093	2.8103	1.9295	0.8332	ω CH(64)
47	809(vw)	811(w)	840	807	4.5212	4.1268	1.5525	0.6466	ω CH(62)
48	746(vw)	754(vw)	788	758	4.0811	5.3778	1.8634	0.6826	ω CH(63)
49	706(w)	708(ms)	743	714	9.8358	9.5697	2.1263	0.6932	bNN(65)
50	599(w)	–	576	554	0.7252	3.7343	2.5853	0.5062	Rasynd(64)
51	–	536(ms)	557	535	1.6292	0.2387	1.7923	0.3284	Rsynd(63)
52	–	458(ms)	431	414	10.2359	1.6621	2.7033	0.2968	Rtrigd(64)
53	–	436(vw)	384	369	0.4410	3.4973	2.9333	0.2557	NH _{2wao} (65)
54	–	358(vw)	356	342	6.2590	0.6101	2.9031	0.2172	Rasynd(66)
55	–	348(w)	343	330	0.6323	1.5636	2.1573	0.1499	tRasynd(60)
56	–	–	300	288	21.7047	1.1649	1.5339	0.0817	tRasynd(61)
57	–	–	280	269	5.5705	0.8495	1.6510	0.0766	tRtrigd(60)
58	–	–	227	218	0.6455	0.0866	1.7196	0.0525	tRasynd(61)
59	–	–	146	140	2.5891	0.6762	2.6655	0.0335	ω NN(59)
60	–	96(ms)	52	50	0.4802	0.0762	1.9138	0.0032	NH _{2wist} (58)

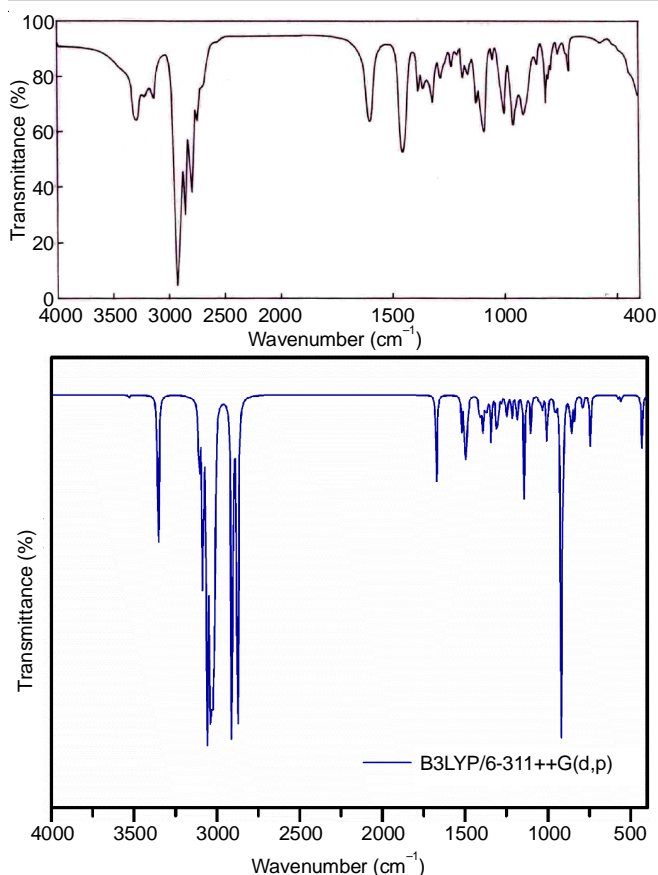


Fig. 2. FT-IR plot for 1-aminohomopiperidine

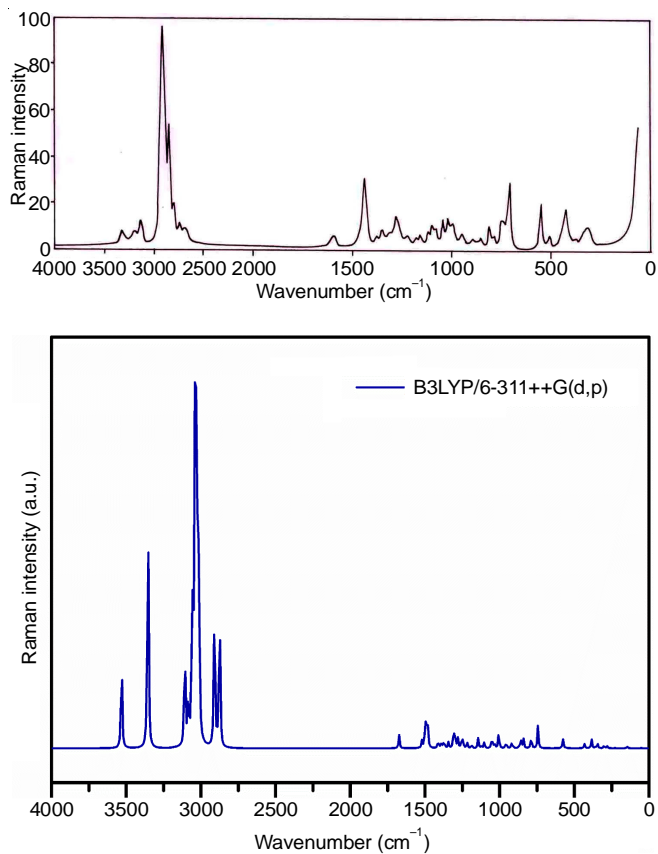


Fig. 3. FT-Raman plot for 1-aminohomopiperidine

CN vibrations: The assignment of CN vibrations is difficult as they may be blended with several groups. The stretching C-N vibrations are distributed within the region 1400-1266 cm^{-1} for heteroaromatic compounds [33]. In 1AHP, the band recognized at 1388, 1357 cm^{-1} in FTIR and 1396 cm^{-1} in FT-Raman spectra are consigned to CN stretching and the equivalent force constant pay about nearly 85% to TED as given in Table-3.

NH₂ vibrations: The NH₂ group has six related vibrations such as symmetric stretch, antisymmetric stretch, rocking, scissoring, twisting and wagging modes. The NH₂ vibrations are obtained in the range from 3500-3300 cm^{-1} for heterocyclic compounds. The NH₂ absorption is definite by the hydrogen bonds and the physical status of the material. Hence, the NH₂ asymmetric vibrations are set up at 3349 cm^{-1} in IR and 3358 cm^{-1} in FT-Raman whereas the corresponding computed band is obtained at 3394 cm^{-1} with TED nearly 98% for 1AHP. The NH₂ scissoring, rocking vibrations are assigned well by the literature results [34].

C-C vibrations: The C-C stretching vibrations contribute main part in the substituted piperidine framework. In general, the C-C stretching frequencies are appeared in the region 1624-726 cm^{-1} [35]. In the present work, experimentally measured peaks at 1498, 1477, 1454, 1409, 1397 cm^{-1} in IR and 1484, 1412 cm^{-1} in Raman have been assigned for CC vibrations, which are supported by the approximately 80-85% of TED. The corresponding scaled DFT wavenumbers have been computed at 1520, 1501, 1499, 1496, 1489 cm^{-1} . The ring CC vibrations are found well within distinctive range and are given in Table-3.

C-H vibrations: The C-H vibrational range [36] always built up in between 3100-3000 cm^{-1} . The scaled DFT frequencies found at 2988, 2966, 2942, 2935, 2922, 2917, 2909, 2905, 2900, 2894, 2795, 2764 cm^{-1} characterizes the C-H stretching vibrational modes (nearly 90% TED) for 1AHP. Likewise, the experimental C-H vibrations have been noted at 3012, 3009, 2999, 2997, 2994, 2964, 2888, 2887, 2878, 2858, 2841, 2832, 2782, 2758 and 2646 cm^{-1} in both the vibrational spectra. In Table-3, the C-H bending [37] vibrations of 1AHP are also recorded.

Molecular electrostatic potential (MEP) surface analysis: MEP surface is used to deliver the potential interactions and that was performed by B3LYP/6-311++G (d,p) basis set [38]. From the MEP study of 1AHP, the red surface depicts the electrostatic negative potential and blue surface represents the electrostatic positive potential as shown in Fig. 4. The negative potential is located around nitrogen atom (N8) which is the probable strongest repulsive site for the electrophilic reactions. The C7 atom is also electronegative since it is arranged to be held nearby nitrogen. The positive potential locates around the hydrogen atoms H10 and H9, which show the strongest attraction for nucleophilic reactions. The MEP of 1AHP describes that the nitrogen atoms in the ring are possible to outbreak the reactive sites.

Electronic spectra analysis: The UV-visible spectra are simulated to recognize the electronic shifts of 1AHP using TD-DFT/B3LYP technique with 6-311++G (d,p) basis set. The

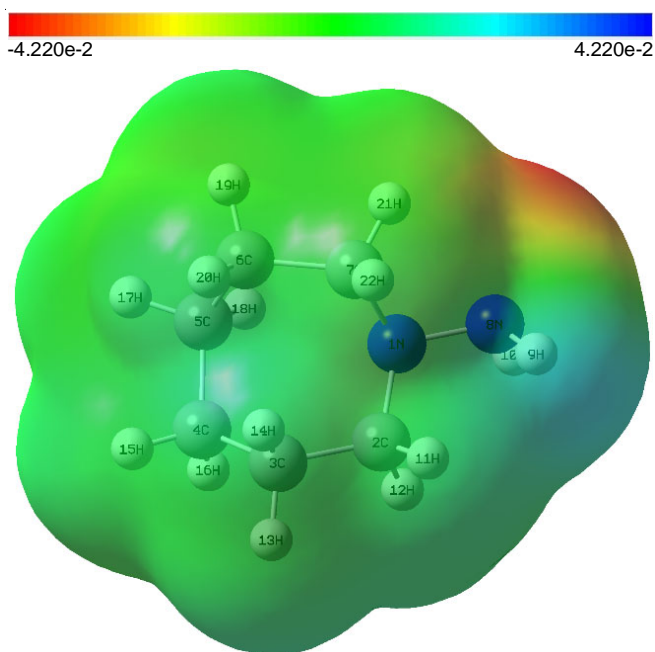


Fig. 4. MEP plot for 1-aminohomopiperidine (1AHP)

TD-DFT design is a beneficial tool for examining the static assets of 1AHP in their excited states [39,40]. The computed UV-Vis spectra of 1AHP are visualized in Fig. 5. Three main excitation energy contributions and the equivalent assignments are provided in Table-4. The strong peak is observed at 223.72 nm with oscillator quality $f = 0.0515$ and energy $E = 5.5419$ eV, which is assigned as $H \rightarrow L+2$ transition ($\pi \rightarrow \pi^*$) with contribution of 96.2%. This $\pi \rightarrow \pi^*$ transition arises due to the hyperconjugation interaction between the amine group and piperidine ring. Another energize state is computed at 249.65 nm with frequency $f = 0.0280$, energy $E = 4.9664$ eV due to $H \rightarrow L$ transition ($\pi \rightarrow \pi^*$ type) by contributions of 91.5%. For 1AHP, the transition $H \rightarrow L+1$ ($\pi \rightarrow \pi^*$ type) is observed at 232.12 nm with oscillator quality $f = 0.0133$ and energy $E = 5.3414$ eV, which contributes 89.1%.

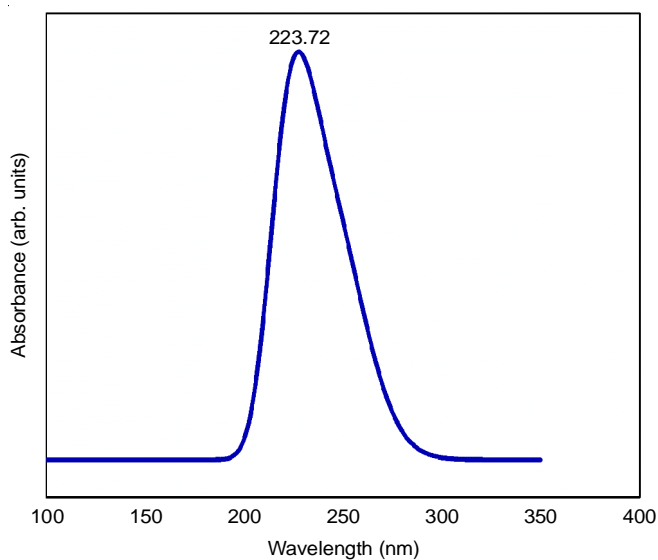


Fig. 5. UV plot for of 1-aminohomopiperidine

TABLE-4 MOLECULAR ORBITAL CONTRIBUTIONS OF 1-AMINOHOMOPIPERIDINE				
TDDFT/ B3LYP/ 6-311++G(d,p) method				
Energy (eV)	Oscillator strength	Computed wavelength (nm)	Major contributions	Assignment
4.9664	0.0280	249.65	H→L (91.5%)	$\pi \rightarrow \pi^*$
5.3414	0.0133	232.12	H→L+1 (89.1%)	$\pi \rightarrow \pi^*$
5.5419	0.0515	223.72	H→L+2 (96.2%)	$\pi \rightarrow \pi^*$

Frontier molecular orbital (FMO) analysis: The significant two molecular orbitals such as highest occupied molecular orbital (HOMO) and the lowest unoccupied molecular orbital (LUMO) are termed the frontier molecular orbitals (FMOs) and considered by their capacity to donate or accept electrons [41]. The HOMO-LUMO orbital energies calculated by B3LYP /6-311++G (d,p) method for 1AHP is shown in Fig. 6. Band gap orbital is determined from the energy variance among the HOMO-LUMO. The obtained HOMO energy value is found as -8.5794 eV that permits to be the excellent electron giver (N-N bond of ring). The LUMO energy is calculated as -2.1649 eV which implies the leading electron acceptor (C-C bond of ring) and computed energy gap is established as 6.4145 eV. FMOs are used to elucidate many molecular parameters by using Koopman's relations [42] and these parameters are shown in Table-5. The molecular information of 1AHP is calculated as chemical hardness (3.2072 eV), electron affinity (2.1649 eV), electronegativity (5.3721 eV), electrophilicity index (4.4991 eV), global softness (0.15589 eV) and chemical potential (-5.3721 eV). The lesser chemical potential and higher electrophilicity index represent the chemical stability of 1AHP.

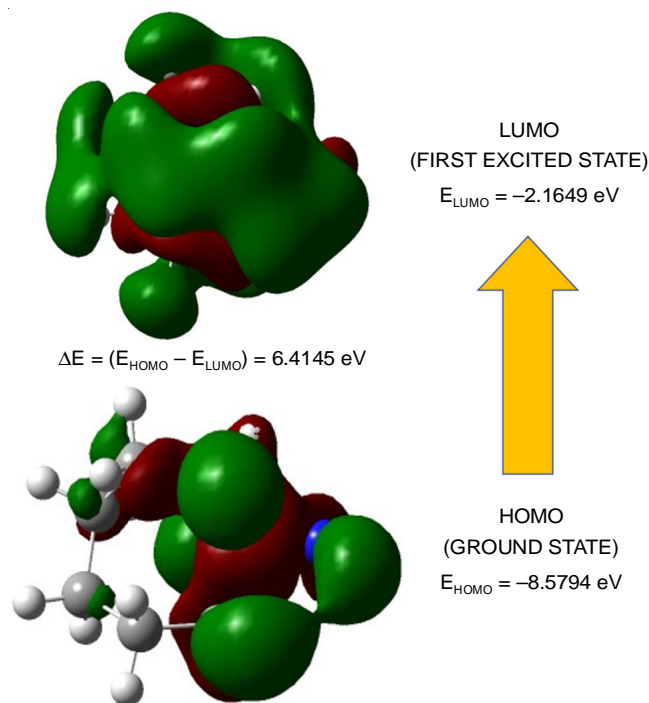


Fig. 6. Frontier molecular orbitals of 1-aminohomopiperidine (1AHP)

TABLE-5
GLOBAL REACTIVITY DESCRIPTORS
FOR 1-AMINOHOMOPIPERIDINE

Molecular properties	B3LYP/6-311++G(d,p)
HOMO (eV)	-8.5794
LUMO (eV)	-2.1649
$\Delta E (E_{\text{HOMO}} - E_{\text{LUMO}})$ (eV)	6.4145
Ionization potential (I) (eV)	8.5794
Electron affinity (A) (eV)	2.1649
Global hardness (η) (eV)	3.2072
Global softness (s) (eV^{-1})	0.1558
Electronegativity (χ) (eV)	5.3721
Chemical potential (μ) (eV)	-5.3721
Global electrophilicity (w) (eV)	4.4991

Mulliken charge analysis: Population study has a central part in the molecular system, since this interrupt dipole moment and electronic assembly. The charge distribution of 1AHP utilizing B3LYP with 6-311++G (d, p) basis set [43] is shown in Fig. 7 and the values are depicted in Table-6. The reactive charges of 1AHP represents the nitrogen N8 (-0.334561) atom and carbon atoms C2 (-0.330927), C3 (-0.292612), C4 (-0.365393), C5 (-0.309249), C6 (-0.218172) and C7 (-0.454187) are highly electronegativity and influenced by their substituents. This higher electronegativity is because of the carbon atoms are attached with the hydrogen atoms. The protonation of C-N bond is repetitive since electronegative repulsion between atoms C7 and N8. The two hydrogen atoms H9 (0.185278) and H10 (0.250313) have better positive charge than the other hydrogen atoms because these hydrogen atoms are located near to nitrogen atom (N8).

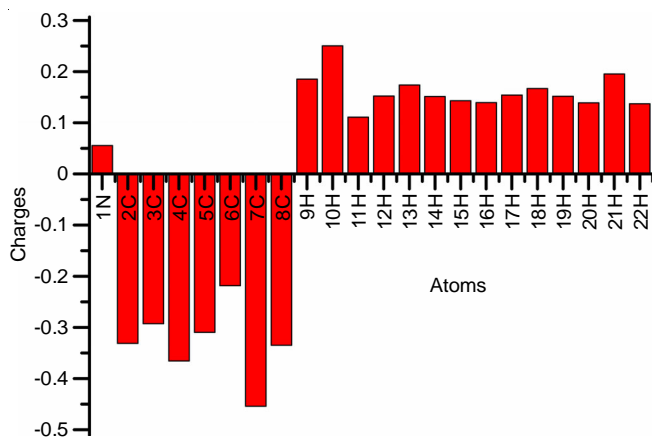


Fig. 7. Mullikan charges for 1-aminohomopiperidine

TABLE-6
MULLIKEN ATOMIC CHARGE
FOR 1-AMINOHOMOPIPERIDINE

Atoms	6-311++G (d,p)	Atoms	6-311++G (d,p)
1N	0.055417	12H	0.152070
2C	-0.330927	13H	0.173591
3C	-0.292612	14H	0.151191
4C	-0.365393	15H	0.143186
5C	-0.309249	16H	0.139517
6C	-0.218172	17H	0.154084
7C	-0.454187	18H	0.166754
8N	-0.334561	19H	0.151472
9H	0.185278	20H	0.138624
10H	0.250313	21H	0.195490
11H	0.110962	22H	0.137154

(0.250313) have better positive charge than the other hydrogen atoms because these hydrogen atoms are located near to nitrogen atom (N8).

NMR analysis: The ^{13}C & ^1H NMR spectra of 1AHP have been obtained by DFT/ B3LYP 6-311++G (d, p) theory with GIAO method. It is the dynamic method to interpret the structure of giant biomolecules [44]. The computed ^{13}C & ^1H shift values of 1AHP in tetramethyl silane (TMS) as a reference are represented in Tables 7 and 8, respectively. In general, the shift series of aromatic carbon atoms are ranging from 100 to 200 ppm [45]. In this work, the computed ^{13}C NMR of the aromatic carbons are noted in between 23.26 and 68.11 ppm. The high electronegative of nitrogen in the piperidine ring influences the carbon atoms and hence the maximum shift of aromatic carbons C2 and C7 are found as 68.11 and 58.11 ppm. The carbon C5 gives the lowermost shift at 23.92 ppm, since it is coupled to the hydrogen atoms H17, H18. Hydrogens connected straight forwardly diminishes shielding and the resonance leads to high wavenumber. From Table-8, the computed signal for H10 attached near to nitrogen atom (N8) has a maximum value of 3.53 ppm. Hydrogens placed closer to electron donor, it rises the shielding and therefore the resonance shifted to a lesser wave-number. In this study, the atoms H13 and H17 have the minimum shift value of 1.33 and 1.32 ppm, respectively.

TABLE-7
 ^{13}C NMR CHEMICAL SHIFTS FOR 1-AMINOHOMOPIPERIDINE

Atoms	Calculated shift (ppm)	Atoms	Calculated shift (ppm)
C2	68.11	C5	23.92
C3	27.44	C6	26.12
C4	28.26	C7	58.11

TABLE-8
 ^1H NMR CHEMICAL SHIFTS FOR 1-AMINOHOMOPIPERIDINE

Atoms	Calculated shift (ppm)	Atoms	Calculated shift (ppm)
H10	3.53	H17	1.32
H11	2.17	H18	2.25
H12	2.94	H19	1.71
H13	1.33	H20	1.41
H14	1.70	H21	3.06
H15	1.43	H22	2.62
H16	1.67		

Natural bonding orbital analysis (NBO): In order to understand the intramolecular charge transfer (ICT) and hydrogen bonding inside the molecule frameworks, NBO analysis has been utilized [46]. In NBO study, the donor-acceptor relations carried out by the second-order Fock matrix [47]. In 1AHP, the NBO investigation is executed using B3LYP/6-311++G(d,p) basis set from NBO 3.1 package employed in Gaussian 09 software and the obtained results are recorded in Table-9. In general, greater the stabilization energy value which associated with more tendency to donate (i) electrons to acceptor (j) orbitals. The ICT interaction from the lone pair electron of N to σ^* is the distinctive feature of a medicinal compound [48,49]. In 1AHP, the solid intramolecular interaction energy is gotten

TABLE-9
SECOND-ORDER PERTURBATION THEORY ANALYSIS OF FOCK MATRIX FOR 1-AMINOHOMOPIPERIDINE BY NBO ANALYSIS

Donor (i)	ED (i) (e)	Acceptor (j)	ED (j) (e)	E(2) ^a (Kcal/mol)	E(j)-E(i) ^b (arb. units)	F(i,j) ^c (arb. units)
σ (N1-N8)	1.98774	σ^* (C2-C3)	0.01873	1.55	1.16	0.038
σ (N1-N8)	1.98774	σ^* (C6-C7)	0.02110	1.36	1.14	0.035
σ (C2-C3)	1.98282	σ^* (N1-N8)	0.01808	2.90	0.92	0.046
σ (C2-C3)	1.98282	σ^* (C4-H15)	0.01204	1.14	1.03	0.031
σ (C2-H11)	1.98456	σ^* (C3-C4)	0.01580	3.35	0.89	0.049
σ (C2-H12)	1.98143	σ^* (N1-C7)	0.02271	3.51	0.86	0.049
σ (C2-H12)	1.98143	σ^* (C3-H14)	0.01703	2.64	0.90	0.044
σ (C3-C4)	1.98454	σ^* (C2-H11)	0.03253	1.41	0.98	0.033
σ (C3-H13)	1.97520	σ^* (N1-C2)	0.03030	3.72	0.85	0.05
σ (C3-H13)	1.97520	σ^* (C4-C5)	0.01650	3.33	0.88	0.048
σ (C3-H14)	1.97746	σ^* (C2-H12)	0.01842	2.64	0.90	0.043
σ (C3-H14)	1.97746	σ^* (C4-H16)	0.01321	2.76	0.90	0.045
σ (C4-C5)	1.98491	σ^* (C3-H13)	0.01032	1.35	1.00	0.033
σ (C4-C5)	1.98491	σ^* (C6-H19)	0.01061	1.24	1.01	0.032
σ (C4-H15)	1.97938	σ^* (C2-C3)	0.01873	3.87	0.87	0.052
σ (C4-H15)	1.97938	σ^* (C5-H18)	0.01556	1.85	0.91	0.037
σ (C4-H16)	1.98118	σ^* (C3-H14)	0.01703	2.83	0.89	0.045
σ (C4-H16)	1.98118	σ^* (C5-C6)	0.01256	2.45	0.88	0.042
σ (C5-C6)	1.98471	σ^* (C4-H16)	0.01321	1.06	1.01	0.029
σ (C5-H17)	1.97954	σ^* (C3-C4)	0.01580	2.54	0.87	0.042
σ (C5-H17)	1.97954	σ^* (C6-C7)	0.02110	3.41	0.85	0.048
σ (C5-H18)	1.98042	σ^* (C4-H15)	0.01204	1.69	0.89	0.035
σ (C5-H18)	1.98042	σ^* (C6-H20)	0.01469	2.92	0.89	0.046
σ (C6-C7)	1.98353	σ^* (N1-N8)	0.01808	2.27	0.90	0.04
σ (C6-C7)	1.98353	σ^* (C5-H17)	0.01213	1.26	1.01	0.032
σ (C6-H19)	1.97963	σ^* (N1-C7)	0.02271	1.37	0.84	0.03
σ (C6-H19)	1.97963	σ^* (C4-C5)	0.01650	3.22	0.87	0.047
σ (C6-H20)	1.98315	σ^* (C5-H18)	0.01556	2.60	0.92	0.044
σ (C7-H21)	1.98171	σ^* (N1-C2)	0.03030	3.70	0.85	0.05
σ (C7-H21)	1.98171	σ^* (C6-H19)	0.01061	1.03	0.91	0.027
σ (C7-H21)	1.98171	σ^* (C6-H20)	0.01469	1.06	0.90	0.028
σ (C7-H22)	1.98941	σ^* (C5-C6)	0.01256	1.48	0.89	0.033
σ (N8-H10)	1.99101	σ^* (N1-C7)	0.02271	2.59	0.99	0.045
LP1(N1)	1.88268	σ^* (C2-H11)	0.03253	15.23	0.66	0.063
LP1(N1)	1.88268	σ^* (C2-H12)	0.01842	12.99	0.69	0.039
LP1(N1)	1.88268	σ^* (C6-C7)	0.02110	2.02	0.65	0.033
LP1(N1)	1.88268	σ^* (C7-H22)	0.03021	12.99	0.68	0.063
LP1(N1)	1.88268	σ^* (N8-H9)	0.02596	6.52	0.69	0.061
LP1(N1)	1.88268	σ^* (N8-H10)	0.00927	2.25	0.71	0.037
LP1(N8)	1.97025	σ^* (N1-C2)	0.03030	5.51	0.69	0.055

from the lone pair electrons of N1 to the σ^* (C2-H11) and σ^* (C2-H22) orbitals, which cause the stabilization energies of 15.23 and 12.99 kcal mol⁻¹, respectively. Furthermore, the significant σ to σ^* charge exchanges lead to the optimistic polarization and that gives more biological activity to 1AHP.

Docking analysis: The docking analyses are used to recognize the right authoritative postures within the binding location of the protein. The *in-silico* analyses exposed that the molecule 1AHP binds well with the breast cancer marker protein ER α (estrogen receptor alpha) [50] as shown in Fig. 8. Their binding energies and interacting residues are reported in Table-10. The ER α play key role in the therapy with inhibitors and there are a set of patients (17%) that do not active to the treatment due to lack of ER α . Triple negative breast cancers

(TNBC) signify a highly aggressive sub-type of breast cancer lacks expression of ER α [51,52]. Selective estrogen receptor modulators (SERMs) bind to ER α can control its transcriptional capabilities in many ways within various estrogen tissue targets. Further, tamoxifen functions as an antagonist to ER α and blocks its signaling pathway in ER α + breast cancer cells [53]. Thus, ER α act as a target protein for breast cancer treatment, they involved in the development of cancer and also cancer inhibition [54]. The present study revealed that 1AHP binds well with ER α (hydrophobic interaction) at Leu 26, Tyr 29, Ser 25, Asp 27, Tyr 10 and ser 20. The binding free energy (ΔG°) for ER α was found to be -6.10 KJ mol⁻¹. From docking studies, it is evident that the inhibition activities of ER α are affected by 1AHP and therefore the highest binding energy

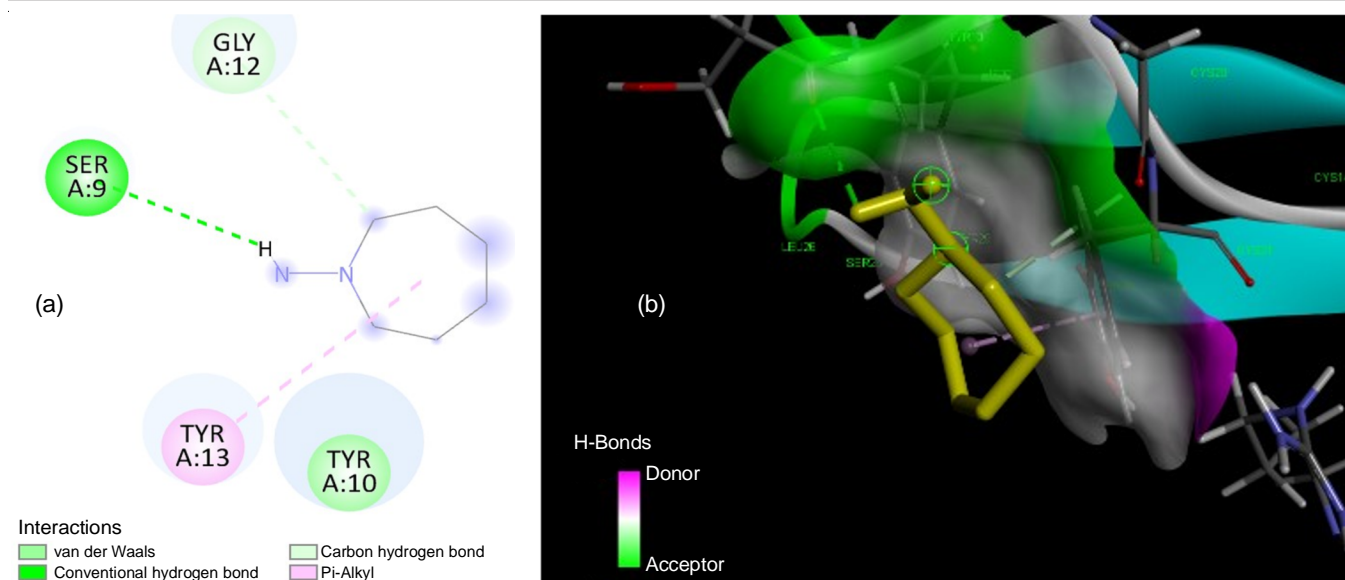


Fig. 8. (a) 2D structure of 1-aminohomopiperidine interacts with the breast cancer ER α protein; (b) Interaction of 1-aminohomopiperidine with the breast cancer marker ER α

TABLE-10a
MOLECULAR DOCKING RESULTS FOR 1-AMINOHOMOPIPERIDINE WITH ER α

Protein	Binding energy	Ligand efficiency	Inhibit constant	Intermol energy	vdw HB dissolve energy	Electrostatic energy	Total internal	Torsional energy	Unbound energy
ER α (estrogen receptor alpha) (PDB ID: 1EPG)	-6.10	-0.56	27.34	-6.84	-6.16	-0.05	-0.09	0.5	-0.04

TABLE-10b
DOCKING CALCULATION SHOWING INTERACTING RESIDUES, BINDING RESIDUES INVOLVED IN H-BONDING TO REPORTED ACTIVE SITES

Protein	Interacted residues	Ligand and protein atom involved in H-bonding
ER α (estrogen receptor alpha) (PDB ID: 1EPG)	TYRA:10, SERA:9, GLYA:12, TYRA:13	SERA:9

has been obtained. So, it is sensible to speculate that the 1AHP might have potent breast cancer activity.

Conclusion

The optimized structural parameters and spectroscopic studies of 1-aminohomopiperidine (1AHP) have been investigated by DFT/B3LYP/6-311++G(d,p) method. Frequencies of normal modes have been analyzed and agree well with the experimental values. The MEP examination shows the responsive bioactive locales of the molecule. The Mulliken distribution and FMOs analysis confirmed the chemical activity of the molecule. The electronic spectra of 1AHP are performed which reflects the frontier molecular orbitals. The computed shifts of ^{13}C & ^1H NMR confirmed the structural information of the molecule. The NBO specifies the intra- and intermolecular charge exchanges of the molecule. The result of docking studies indicates that 1AHP might have potential development for breast cancer marker.

CONFLICT OF INTEREST

The authors declare that there is no conflict of interests regarding the publication of this article.

REFERENCES

- Y. Feng, M. Spezia, S.Huang, C. Yuan, Z. Zeng, L. Zhang, X. Ji, W. Liu, B. Huang, W. Luo, B. Liu, Y. Lei, S. Du, A. Vuppalapati, H.H. Luu, R.C. Haydon, T.-C. He and G. Ren, *Genes Dis.*, **5**, 77 (2018); <https://doi.org/10.1016/j.gendis.2018.05.001>
- F. Bray, J.-S. Ren, E. Masuyer and J. Ferlay, *Int. J. Cancer*, **132**, 1133 (2013); <https://doi.org/10.1002/ijc.27711>
- H. Sung, J. Ferlay, R.L. Siegel, M. Laversanne, I. Soerjomataram, A. Jemal and F. Bray, *CA Cancer J. Clin.*, **71**, 209 (2021); <https://doi.org/10.3322/caac.21660>
- M. Mareel and A. Leroy, *Physiol. Rev.*, **83**, 337 (2003); <https://doi.org/10.1152/physrev.00024.2002>
- J. Cummings, T.H. Ward, M. Ranson and C. Dive, *Biochim. Biophys. Acta*, **1705**, 53 (2004); <https://doi.org/10.1016/j.bbcan.2004.09.005>
- J. Wesche, K. Haglund and E.M. Haugsten, *Biochem. J.*, **437**, 199 (2011); <https://doi.org/10.1042/BJ20101603>
- R.C. DeConti, *Semin. Oncol.*, **39**, 145 (2012); <https://doi.org/10.1053/j.seminoncol.2012.01.002>
- A.G. Glass, J.V. Lacey, J.D. Carreon and R.N.J. Hoover, *J. Natl. Cancer Inst.*, **99**, 1152 (2007); <https://doi.org/10.1093/jnci/djm059>
- O. Gluz, C. Liedtke, N. Gottschalk, L. Pusztai, U. Nitz and N. Harbeck, *Ann. Oncol.*, **20**, 1913 (2009); <https://doi.org/10.1093/annonc/mdp492>

10. O.K. Abel and S. Banjo, *New York Science J.*, **9**, 58 (2016); <https://doi.org/10.7537/marsnys09061610>
11. M.B. Smith and J. March, *March's Advanced Organic Chemistry Reactions, Mechanisms and Structure*, John Wiley & Sons (2007).
12. G. Brahmachari, C. Choo, P. Ambure and K. Roy, *Bioorg. Med. Chem.*, **23**, 4567 (2015); <https://doi.org/10.1016/j.bmc.2015.06.005>
13. R. Saxena, V. Chandra, M. Manohar, U. Debnath, Y.S. Prabhakar, K.S. Saini, K. Hajela, R. Konwar, S. Kumar, K. Megu, B.G. Roy and A. Dwivedi, *PLoS One*, **8**, e66246 (2013); <https://doi.org/10.1371/journal.pone.0066246>
14. S.N. Mokale, P.N. Dube, S.A. Bhavale, I. Sayed, A. Begum, M.C. Nevase, V.R. Shelke and A. Mujaheed, *Med. Chem. Res.*, **24**, 1842 (2015); <https://doi.org/10.1007/s00044-014-1266-8>
15. A. Singh, S. Goyal, S. Jamal, B. Subramani, M. Das, N. Admane and A. Grover, *Struct. Chem.*, **27**, 993 (2016); <https://doi.org/10.1007/s11224-015-0697-2>
16. N. Karaman, Y. Sicak, T. Taskin-Tok, M. Öztürk, A. Karakütük-Iyidogan, M. Dikmen, B. Koçyigit-Kaymakçioğlu and E.E. Oruç-Emre, *Eur. J. Med. Chem.*, **124**, 270 (2016); <https://doi.org/10.1016/j.ejmech.2016.08.037>
17. P. Trivedi, N. Adhikari, S.A. Amin, Y. Bobde, R. Ganesh, T. Jha and B. Ghosh, *Eur. J. Pharm. Sci.*, **138**, 105046 (2019); <https://doi.org/10.1016/j.ejps.2019.105046>
18. M.E. Vaschetto, B.A. Retamal and A.P. Monkman, *J. Mol. Struct. THEOCHEM*, **468**, 209 (1999); [https://doi.org/10.1016/S0166-1280\(98\)00624-1](https://doi.org/10.1016/S0166-1280(98)00624-1)
19. S. Premkumar, A. Jawahar, T. Mathavan, M.K. Dhas, V.G. Sathe and A.M. Franklin Benial, *Spectrochim. Acta A Mol. Biomol. Spectrosc.*, **129**, 74 (2014); <https://doi.org/10.1016/j.saa.2014.02.147>
20. T. Lengauer and M. Rarey, *Curr. Opin. Struct. Biol.*, **6**, 402 (1996); [https://doi.org/10.1016/S0959-440X\(96\)80061-3](https://doi.org/10.1016/S0959-440X(96)80061-3)
21. M.J. Frisch, G.W. Trucks, H.B. Schlegel, G.E. Scuseria, M.A. Robb, J.R. Cheesman, V.G. Zakrzewski, J.A. Montgomery Jr., R.E. Stratmann, J.C. Burant, S. Dapprich, J.M. Millam, A.D. Daniels, K.N. Kudin, M.C. Strain, O. Farkas, J. Tomasi, V. Barone, M. Cossi, R. Cammi, B. Mennucci, C. Pomelli, C. Adamo, S. Clifford, J. Ochterski, G.A. Petersson, P.Y. Ayala, Q. Cui, K. Morokuma, N. Rega, P. Salvador, J.J. Dannenberg, D.K. Malich, A.D. Rabuck, K. Raghavachari, J.B. Foresman, J. Cioslowski, J.V. Ortiz, A.G. Baboul, B.B. Stetanov, G. Liu, A. Liashenko, P. Piskorz, I. Komaromi, R. Gomperts, R.L. Martin, D.J. Fox, T. Keith, M.A. Al-Laham, C.Y. Peng, A. Nanayakkara, M. Challacombe, P.M.W. Gill, B. Johnson, W. Chen, M.W. Wong, J.L. Andres, C. Gonzalez, M. Head-Gordon, E.S. Replogle and J.A. Pople, GAUSSIAN 09, Revision A.11.4, Gaussian, Inc, Pittsburgh, PA (2009).
22. A.D. Becke, *J. Chem. Phys.*, **98**, 5648 (1993); <https://doi.org/10.1063/1.464913>
23. C. Lee, W. Yang and R.G. Parr, *Phys. Rev.*, **37**, 785 (1988); <https://doi.org/10.1103/PhysRevB.37.785>
24. M. Castellà-Ventura, E. Kassab, G. Buntinx and O. Poizat, *Physiol. Chem. Phys.*, **2**, 4682 (2000); <https://doi.org/10.1039/b006459j>
25. D.C. Young, *Computational Chemistry: A Practical Guide for Applying Techniques to Real World Problems (Electronic)*, John Wiley & Sons Ltd.: New York (2001).
26. J.K. Milam, Gauss View, Version 5, Ray Dennington, Semichem Inc, Shawnee K S Mission, vol. 7, p. 41 (2009).
27. MOLVIB, (V.7.0), Calculation of Harmonic Force Fields and Vibrational Modes of Molecules, QCPE Program No. 807, (2002).
28. U.P. Mohan, S. Kunjiappan, P.B.T. Pichiah and S. Arunachalam, *3 Biotech.*, **11**, 15 (2021); <https://doi.org/10.1007/s13205-020-02530-9>
29. O. Trott and A.J. Olson, *J. Comput. Chem.*, **31**, 455 (2009); <https://doi.org/10.1002/jcc.21334>
30. B.L. Narayana, D.P. Kishore, C. Balakumar, K.V. Rao, R. Kaur, A.R. Rao, J. Murthy and M. Ravikumar, *Chem. Biol. Drug Des.*, **79**, 674 (2012); <https://doi.org/10.1111/j.1747-0285.2011.01277.x>
31. A.D. Bond, J.E. Davies and S. Parsons, *Acta Crystallogr. C*, **64**, o543 (2008); <https://doi.org/10.1107/S0108270108026012>
32. M.K. Ahmed and B.R. Henry, *J. Phys. Chem.*, **90**, 1737 (1986); <https://doi.org/10.1021/j100400a002>
33. M. Arivazhagan, S. Jeyavijayan and J. Geethapriya, *Spectrochim. Acta A Mol. Biomol. Spectrosc.*, **104**, 14 (2013); <https://doi.org/10.1016/j.saa.2012.11.032>
34. Y. Yamada, J. Okano, N. Mikami and T. Ebata, *J. Chem. Phys.*, **123**, 124316 (2005); <https://doi.org/10.1063/1.2039087>
35. G. Sivaraj, N. Jayamani and V. Siva, *J. Mol. Struct.*, **1240**, 130530 (2021); <https://doi.org/10.1016/j.molstruc.2021.130530>
36. V. Siva, S. Suresh Kumar, M. Suresh, M. Raja, S. Athimoolam and S. Asath Bahadur, *J. Mol. Struct.*, **1133**, 163 (2017); <https://doi.org/10.1016/j.molstruc.2016.11.088>
37. V. Siva, S.S. Kumar, A. Shameem, M. Raja, S. Athimoolam and S.A. Bahadur, *J. Mater. Sci. Mater. Electron.*, **28**, 12484 (2017); <https://doi.org/10.1007/s10854-017-7070-8>
38. O. Noureddine, N. Issaoui and O. Al-Dossary, *J. King Saud Univ. Sci.*, **33**, 101248 (2021); <https://doi.org/10.1016/j.jksus.2020.101248>
39. S. Jeyavijayan and P. Murugan, *Asian J. Chem.*, **33**, 83 (2020); <https://doi.org/10.14233/ajchem.2021.22922>
40. N. Sundaraganesan, G. Elango, C. Meganathan, B. Karthikeyan and M. Kurt, *Mol. Simul.*, **35**, 705 (2009); <https://doi.org/10.1080/08927020902873992>
41. S. Jeyavijayan, M. Ramuthai and P. Murugan, *Asian J. Chem.*, **33**, 2313 (2021); <https://doi.org/10.14233/ajchem.2021.23308>
42. O. Noureddine, N. Issaoui, M. Medimagh, O. Al-Dossary and H. Marouani, *J. King Saud Univ. Sci.*, **33**, 101334 (2021); <https://doi.org/10.1016/j.jksus.2020.101334>
43. B. Pramodh, P. Naresh, S. Naveen, N.K. Lokanath, S. Ganguly, J. Panda, S. Murugesan, A.V. Raghu and I. Warad, *Chem. Data Coll.*, **31**, 100587 (2021); <https://doi.org/10.1016/j.cdc.2020.100587>
44. K. Rastogi, M.A. Palafox, R.P. Tanwar and L. Mittal, *Spectrochim. Acta A Mol. Biomol. Spectrosc.*, **58**, 1987 (2002); [https://doi.org/10.1016/S1386-1425\(01\)00650-3](https://doi.org/10.1016/S1386-1425(01)00650-3)
45. J. Luque, J.M. Lopez and M. Orozco, *Theor. Chem. Acc.*, **103**, 343 (2000); <https://doi.org/10.1007/s002149900013>
46. M. Nsangou, Z. Dhaouadi, N. Jaïdane and Z. Ben Lakhdar, *J. Mol. Struct. THEOCHEM*, **819**, 142 (2007); <https://doi.org/10.1016/j.theochem.2007.05.038>
47. S.P. Vijaya Chamundeeswari, E.J. Jebaseelan Samuel and N. Sundaraganesan, *Mol. Simul.*, **38**, 987 (2012); <https://doi.org/10.1080/08927022.2012.682279>
48. J. Cerny and P. Hobza, *Phys. Chem. Phys.*, **9**, 5291 (2007); <https://doi.org/10.1039/b704781a>
49. R. Mohamed Asath, R. Premkumar, T. Mathavan and A.M. Franklin Benial, *J. Mol. Struct.*, **1143**, 415 (2017); <https://doi.org/10.1016/j.molstruc.2017.04.117>
50. B.J. Deroo and K.S. Korach, *J. Clin. Invest.*, **116**, 561 (2006); <https://doi.org/10.1172/JCI27987>
51. W.J. Irvin Jr. and L.A. Carey, *Eur. J. Cancer*, **44**, 2799 (2008); <https://doi.org/10.1016/j.ejca.2008.09.034>
52. J.S. Reis-Filho and A.N. Tutt, *Histopathology*, **52**, 108 (2008); <https://doi.org/10.1111/j.1365-2559.2007.02889.x>
53. L. Björnström and M. Sjöberg, *Mol. Endocrinol.*, **19**, 833 (2005); <https://doi.org/10.1210/me.2004-0486>
54. Y. Liu, H. Ma and J. Yao, *OncoTargets Ther.*, **13**, 2183 (2020); <https://doi.org/10.2147/OTT.S236532>